The American Journal of Pathology, Vol. 169, No. 5, November 2006

DOI: 10.2353/ajpath.2006.060169

Cardiovascular, Pulmonary and Renal Pathology

Inhibition of p38 Mitogen-Activated Protein Kinase and Transforming Growth Factor-β1/Smad Signaling Pathways Modulates the Development of Fibrosis in Adriamycin-Induced Nephropathy

Jinhua Li,* Naomi Vittoria Campanale,* Rong Jiao Liang,* James Antony Deane,*† John Frederick Bertram,† and Sharon Denise Ricardo*†

From Monash Immunology and Stem Cell Laboratories and the Department of Anatomy and Cell Biology,† Monash University, Victoria, Australia*

Inflammation and fibrogenesis are the two determinants of the progression of renal fibrosis, the common pathway leading to end-stage renal disease. The p38 mitogen-activated protein kinase (MAPK) and transforming growth factor (TGF)-β1/Smad signaling pathways play critical roles in inflammation and fibrogenesis, respectively. The present study examined the beneficial renoprotective effect of combination therapy using the p38 MAPK pathway inhibitor (SB203580) and a TGF-β receptor I (ALK5) inhibitor (ALK5I) in a mouse model of adriamycin (ADR) nephrosis. The p38 MAPK and TGF-β1/Smad2 signaling pathways were activated in ADR-induced nephropathy in a sequential time course manner. Two weeks after ADR injection, the combined administration of SB203580 (1 mg/kg/24 hours) and ALK5I (1 mg/kg/24 hours) markedly reduced p38 MAPK and Smad2 activities. Moreover, the co-administration of SB203580 and ALK5I to ADR-injected mice resulted in a down-regulation of total and active TGF-β1 production, reduced myofibroblast accumulation, and decreased expression of collagen type IV and fibronectin. In these mice, retardation in the development of glomerulosclerosis and interstitial fibrosis was observed. In conclusion, although p38 MAPK and TGF-β1/Smad signaling pathways are distinct they coordinate the progression of renal fibrosis in ADR nephrosis. The co-administration of a p38 MAPK inhibitor and an ALK5 inhibitor may have potential applications in the treatment of renal fibrosis. ***(Am J Pathol 2006, 169:1527–1540; DOI: 10.2353/ajpath.2006.060169)***

Renal fibrosis is a major determinant of loss of renal function leading to end-stage renal disease regardless of the nature of the initial insult. The progression of renal fibrosis is a complex process involving various intricate intracellular signaling pathways. An improved understanding of the role that signaling pathways play in renal fibrogenesis will allow for more rational interventions based on their manipulations. The p38 mitogen-activated protein kinase (MAPK) pathway and transforming growth factor (TGF)-β1/Smad signaling pathway are important intracellular signaling pathways involved in the production of proinflammatory and profibrotic mediators and the synthesis and deposition of extracellular matrix (ECM) products. However, the mechanisms of how p38 MAPK and TGF-β1/Smad signaling coordinate the development of renal fibrosis *in vivo* remain unclear.

p38 MAPK, extracellular signal-regulated kinase (ERK), c-Jun N-terminal kinase (JNK)/stress-activated protein kinase-1, and ERK5/big MAP kinase 1 (BMK1) represent central kinases that typically transmit signals generated by cytokines, growth factors, and environmental stress.[1] p38 MAPK is involved in inflammation, cell cycle, growth, differentiation, and induction of cell death.[2] Cytokines and environmental stresses, such as UV irradiation and oxidative stress can activate the MAPK cascade, a series of three protein kinases: a MAPK and two upstream components, MAPK kinase (MAPKK) and MAPKK kinase (MAPKKK). This rapid cascade of sequential kinase phosphorylation results in dual phosphorylation of the Tyr-X-Thr motif of the p38 MAPK (p-p38).[3]

Supported by the Australian Kidney Foundation, the Australian National Health and Medical Research Foundation, and Kidney Health Australia (Bootle Bequest).

Accepted for publication July 20, 2006.

J.L. is the recipient of a Chinese Government Scholarship for Outstanding Overseas Students and a Monash Graduate Scholarship.

Address reprint requests to Sharon D. Ricardo, Ph.D., Monash Immunology and Stem Cell Laboratories, Monash University, Clayton, Victoria 3800, Australia. E-mail: sharon.ricardo@med.monash.edu.au.

The dual phosphorylated p38 MAPK then translocates to the nucleus and activates a variety of transcription factors by phosphorylation, such as ATF-2 (p-ATF-2).[4]

Activation of p38 MAPK can induce the production and secretion of proinflammatory cytokines such as interleukin-1β and tumor necrosis factor-α (TNF-α).[5] In turn, interleukin-1β and TNF-α can activate p38 MAPK, which leads to autocrine and paracrine promotion of an inflammatory response that exacerbates kidney injury.[6,7] Increased activity of p38 MAPK has been observed in patients suffering from inflammatory bowel disease, human diabetic nephropathy, and glomerulonephritis.[8–10] Preclinical studies show that blockade of p38 MAPK with various p38 MAPK kinase inhibitors is efficacious in several disease models, including arthritis and other joint diseases, septic shock, myocardial injury, and kidney injury.[11–13]

TGF-β1 plays a key role in renal fibrosis in both experimental and human kidney diseases.[14,15] TGF-β1 binds to the constitutively active TGF-β type II receptor (TGF-RII), which in turn recruits, phosphorylates, and activates TGF-β type I receptor (TGFRI, ALK5). The active form of TGFRI then phosphorylates Smad2 and Smad3 to form a hetero-oligomeric complex with Smad4, which translocates into the nucleus to regulate transcription of target genes. Increased Smad2 and Smad3 activities have been observed in patients with diabetic nephropathy and glomerulonephritis as well as experimental models of renal disease.[16] There is increasing evidence that blockade of TGF-β1 action can ameliorate renal fibrosis.[14,17–20] TGF-β1/Smad signaling pathways are central to the progression of renal fibrosis, and inhibition of the TGF-β1/Smad signaling pathway may offer a therapeutic treatment for renal fibrosis.

The activities of p38 MAPK and TGF-β1/Smad signaling are up-regulated in nephropathy and play critical roles in inflammation and fibrogenesis, respectively. This study evaluates the therapeutic benefits of combined therapy using SB203580 and ALK5 inhibitor (ALK5I), inhibitors of the p38 MAPK and TGF-β1/Smad signaling pathways, respectively, in a mouse model of adriamycin (ADR)-induced nephropathy. The co-administration of SB203580 and ALK5I afforded marked renoprotection and reduced the development of renal fibrosis in mice with ADR nephropathy compared with the separate administration of these factors. These results clearly demonstrate that the p38 MAPK and TGF-β1/Smad2 signaling pathways, although distinct, play a coordinated role in the progression of renal fibrosis.

Materials and Methods

Experimental Animals

At 8 weeks of age, BALB/c male mice (25 to 30 g body weight) received a single intravenous injection of ADR (10.5 mg/kg; Sigma, St. Louis, MO).[21] Control animals were administered an equivalent intravenous volume of normal saline vehicle (NS). ADR or NS mice were sacrificed at 24 hours, 72 hours, and 2 weeks after injection (n = 6/group/time point). A preliminary experiment was performed to determine the effective dose range of SB203580 and ALK5I in ADR-induced nephropathy. A dose curve of SB203580 and ALK5I ranging from 0.25 to 2 mg/kg/day was administered to control and ADR-injected mice (10 groups/n = 3 mice each). Based on the results from this study, ADR-injected mice receiving SB203580 (1 mg/kg/day) + ALK5I (1 mg/kg/day) achieved maximal renoprotective effects without obvious side effects. Compared with vehicle alone (dimethyl sulfoxide), SB203580 (2 mg/kg/day) alone or ALK5I (2 mg/kg/day) alone did not improve kidney function when compared with SB203580 (1 mg/kg/day) alone or ALK5I (1 mg/kg/day) alone, respectively. Therefore, in the present study, to test the beneficial role of p38 MAPK and/or TGF-βRI/Smad inhibitors, 2 weeks after ADR injection mice were treated with the same volume of vehicle, SB203580 (Calbiochem, La Jolla, CA), and/or ALK5I (Calbiochem) delivered by implantation of Alzet (Durect Corp., Cupertino, CA) osmotic pumps until the experimental end point. Dosages were: SB203580 (1 mg/kg/day), ALK5I (1 mg/kg/day), or combination therapy of SB203580 (1 mg/kg/day) + ALK5I (1 mg/kg/day), respectively (n = 6/group). Mice were sacrificed 4 weeks after ADR or NS injection. The kidneys were collected from each animal, and each kidney was divided into three parts: one part for Western blotting and active and total TGF-β1 measurement, one part for 10% buffered formalin fixed, paraffin-embedded tissue, and one part for 4% paraformaldehyde-fixed, OCT-embedded tissue. All experiments were performed with the approval of the Animal Care and Research Advisory Committee, Monash University, Clayton, VIC, Australia.

Measurement of Proteinuria and Creatinine

All mice were acclimated in metabolic cages with free access to food and water for collection of 24-hour urine samples. Measurement of urine protein and creatinine were determined using a detergent compatible protein assay kit (Bio-Rad, Hercules, CA) and creatinine assay kit (Cayman Chemical, Ann Arbor, MI) according to instructions. Proteinuria was normalized for creatinine excretion. Blood samples taken from mice at the time of sacrifice were used to determine serum creatinine levels using the creatinine assay kit.

Antibodies

The following antibodies were used for Western blot analysis and/or immunohistochemistry: rabbit anti-phospho p38 (p-p38) raised against the dual phosphorylated tyrosine and threonine residues of the p38 peptide, rabbit anti-fibronectin (Sigma Chemical Co., Castle Hill, Australia); mouse anti-α-smooth muscle actin (α-SMA; Sigma Chemical Co.), mouse anti-β-tubulin (Sigma-Aldrich, St. Louis, MO), rabbit anti-phospho ATF-2 (p-ATF2; Cell Signaling Technology, Beverly, MA), goat anti-collagen type IV (Southern Biotechnology, Birmingham, AL), mouse anti-TGF-β1 (R&D Systems, Minneapolis, MN), and mouse anti-glyceraldehyde 3-phosphate dehydrogenase (GAPDH; Chemicon, Temecula, CA). Peroxidase-conjugated rabbit anti-goat and goat anti-rabbit IgG and horseradish peroxi-

dase-conjugated goat anti-mouse IgG were purchased from Sigma-Aldrich.

Western Blot Analysis

At 24 hours, 72 hours, and 2 weeks after ADR injection, or 4 weeks after ADR injection with/without treatment, the kidneys were homogenized and suspended in 0.4 ml of lysis buffer containing 10 mmol/L Tris-HCL, pH 7.4, 1% Triton X-100, 0.5% deoxycholate, 1 mmol/L phenylmethyl sulfonyl fluoride, and 10% proteinase inhibitor (Roche, Castle Hill, Australia). Protein concentration estimations were performed with a detergent-compatible protein assay kit (Bio-Rad), and 50 μg of total protein was loaded per well and separated by sodium dodecyl sulfate-polyacrylamide gel electrophoresis on a 10% polyacrylamide gel. Gels were electroblotted onto a polyvinylidene difluoride membrane (Roche). Blots were incubated with either anti-p-p38 (1:1000), anti-p-Smad2 (1:1000), anti-α-SMA (1:10000), anti-collagen type IV (1:1000), or anti-fibronectin (1:4000) in 5% bovine serum albumin in wash buffer overnight at 4°C. Blots were then incubated with peroxidase-conjugated goat anti-rabbit (1:40,000), goat anti-mouse (1:20,000), or rabbit anti-goat IgG (1:20,000) for 1 hour at room temperature, and bound antibody was detected by ECL Plus (Amersham, Little Chalfont, UK) and captured on autoradiography film (Amersham). To confirm protein levels loaded, membranes were reprobed by anti-β-tubulin (1:10,000) or anti-GAPDH (1:10,000). Densitometry analysis was performed by a Gel Pro analyzer program (Media Cybernetics, Silver Spring, MD).

Histology and Immunohistochemistry

Renal histology was examined in 10% buffered formalin-fixed, paraffin-embedded tissue sections (4 μm) stained with periodic acid-Schiff (PAS) and Masson's trichrome. The degrees of glomerulosclerosis and interstitial fibrosis were measured[22] using Image J software (*http://rsb.info.nih.gov/ij/*). The percentage of glomerulosclerosis was calculated by dividing the total area of PAS-positive staining in the glomerulus by the total area of the glomerulus. Interstitial fibrosis was quantified by dividing the area of trichrome-stained interstitium by the total cortical area. The mean value of 20 randomly selected glomeruli or five cortical fields was determined for each section. Five sections were selected from each kidney.

Immunohistochemical staining was performed as described previously.[23] In brief, sections were microwave oven-heated in a 10 mmol/L citrate buffer (pH 6.0) for 10 minutes. All sections were washed in phosphate-buffered saline (PBS), blocked with 10% normal goat serum plus 10% fetal calf serum in PBS for 30 minutes at room temperature, and incubated overnight at 4°C with anti-p-p38, anti-p-ATF, anti-p-Smad2, anti-α-SMA, anti-F4/80, or anti-TGF-β1 in 1% bovine serum albumin in PBS. Sections were subsequently washed in PBS, endogenous peroxidase inactivated in 3% H_2O_2 in methanol for 20 minutes, incubated with biotin-conjugated goat anti-mouse, goat anti-rabbit, or rabbit anti-goat IgG for 25 minutes, and then followed by ABC kit (Vector Laboratories, Burlingame, CA) and developed with 3,3-diamenobenzidine (Sigma).

Quantitative assessment of the expression of p-Smad2 and p-p38 MAPK signaling pathways in glomerular and tubulointerstitial compartments and infiltrating macrophages was performed as described previously.[23] Nuclear profiles localized for p-Smad2 and p-ATF2 staining were counted in 20 representative glomerular cross-sections or 20 representative high-power ($\times$400 magnification) fields within the tubulointerstitium and expressed as the percentage of positive cells/total cell numbers. The number of infiltrating interstitial macrophages was quantified in 20 nonoverlapping cortical fields and expressed as cells per mm^2 of cortical interstitium.

Confocal Microscopy Analysis

For immunofluorescence, tissues were fixed in 4% paraformaldehyde (Sigma-Aldrich) for 8 hours, transferred to PBS containing 30% sucrose for overnight incubation at 4°C, embedded in O.C.T. (TissueTek, Tokyo, Japan) and stored at −80°C. Frozen sections were cut (5 μm) using a cryostat (Leica, Wetzlar, Germany), blocked with 2% bovine serum albumin in PBS, and incubated with goat anti-collagen type IV (1:400) for 60 minutes at room temperature. Sections were probed with chicken anti-goat Alexa Fluor 647 conjugate (1:2000; Molecular Probes, Eugene, OR), counterstained with 4,6-diamidino-2-phenylindole and mounted with fluorescent mounting medium (DakoCytomation, Glostrup, Denmark). Sections were analyzed with an Olympus Fluoview 1000 confocal microscope (Olympus, Tokyo, Japan), FV10-ASW software (version 1.3c; Olympus) and oil UPLFL $\times$60 objective (NA 1.25; Olympus). Contrast and brightness of the images were further adjusted in Adobe Photoshop 7.0 (Adobe Systems, Inc., San Jose, CA). The percentage of staining area of collagen IV was calculated by dividing the total area of collagen IV-positive staining by the total cortical area.

Measurement of TGF-β1 in Renal Tissues

Total and active TGF-β1 levels in renal tissues were analyzed quantitatively by enzyme-linked immunosorbent assay kits (R&D System Inc.), according to the manufacturer's instructions. Protein samples were acidified with 1 mol/L HCl and neutralized with 1.2 mol/L NaOH/0.5 mol/L 4-(2-hydroxyethyl)-1-piperazineethanesulfonic acid to assay for the amount of total (the sum of latent and active) TGF-β1. The concentration of active TGF-β1 protein was analyzed on samples that were not acidified, whereas the levels of latent TGF-β1 protein were derived as total activity − active (preactivated).

Statistical Analyses

Data are means ± SD with statistical analyses performed using one-way analysis of variance from GraphPad Prism

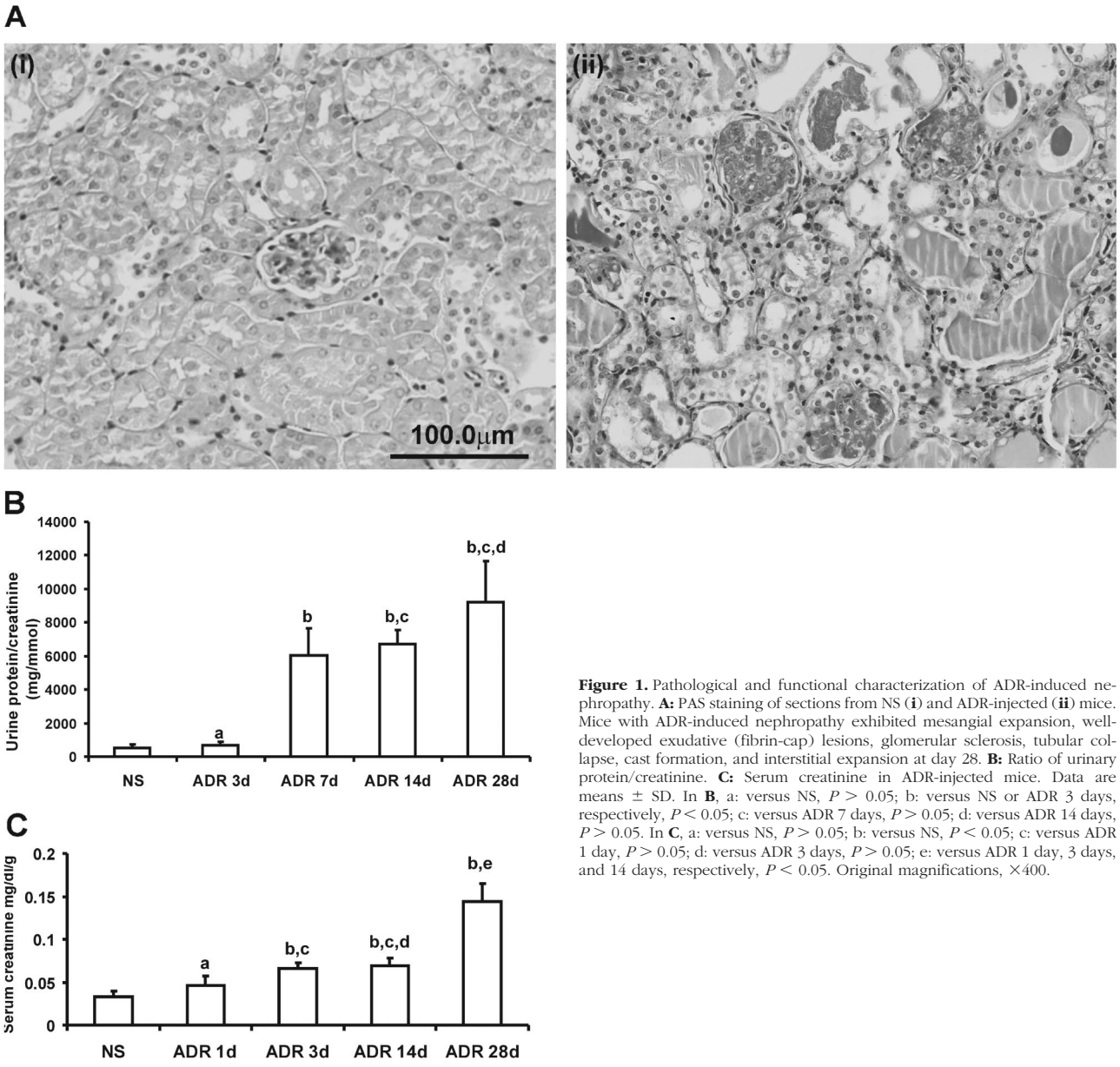

Figure 1. Pathological and functional characterization of ADR-induced nephropathy. **A:** PAS staining of sections from NS (**i**) and ADR-injected (**ii**) mice. Mice with ADR-induced nephropathy exhibited mesangial expansion, well-developed exudative (fibrin-cap) lesions, glomerular sclerosis, tubular collapse, cast formation, and interstitial expansion at day 28. **B:** Ratio of urinary protein/creatinine. **C:** Serum creatinine in ADR-injected mice. Data are means ± SD. In **B**, a: versus NS, $P > 0.05$; b: versus NS or ADR 3 days, respectively, $P < 0.05$; c: versus ADR 7 days, $P > 0.05$; d: versus ADR 14 days, $P > 0.05$. In **C**, a: versus NS, $P > 0.05$; b: versus NS, $P < 0.05$; c: versus ADR 1 day, $P > 0.05$; d: versus ADR 3 days, $P > 0.05$; e: versus ADR 1 day, 3 days, and 14 days, respectively, $P < 0.05$. Original magnifications, ×400.

3.0 (GraphPad Software, Inc., San Diego, CA) and post-test Tukey analysis as required.

Results

Characterization of ADR-Induced Nephrosis

PAS staining showed that administration of ADR to mice resulted in severe glomerular and tubulointerstitial injury, glomerulosclerosis, and interstitial fibrosis (Figure 1A). Proteinuria was evident by 7 days after ADR administration and remained at a similar level throughout the study period (Figure 1B) with increased levels of serum creatinine also observed (Figure 1C).

p38 MAPK and Smad2 Pathway Activation in ADR-Induced Nephrosis

The administration of ADR to mice resulted in an acute activation of p38 MAPK and a later up-regulation of p-Smad2 during the early inflammation phase in the progression of kidney fibrosis. The elevated protein expression of phosphorylated-p38 (p-p38) was demonstrated by Western blotting in which a 1.5-, 2-, and 4-fold increase in p-p38 was observed in the kidneys of ADR-injected mice at 1, 3, and 14 days, respectively, compared with NS mice (Figure 2A, i and ii).

The expression of p-Smad2 was demonstrated by Western blotting with a 0.9-, 1.1-, and 4-fold increase in the kidneys of ADR-injected mice at 1, 3, and 14 days,

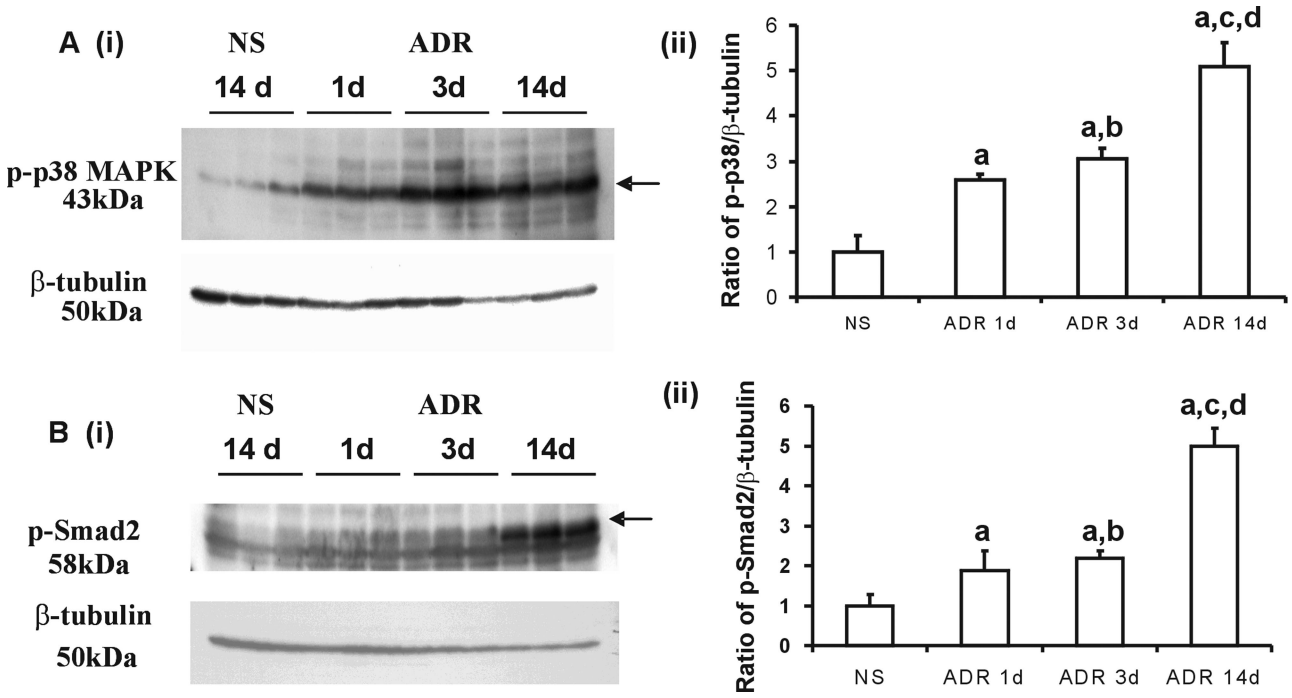

Figure 2. Phospho-Smad2 and Phospho-p38 MAPK are up-regulated in ADR nephropathy. **A** and **B:** Increase in p-p38 and p-Smad2 in ADR-treated kidneys. Whole kidney lysates from normal mouse kidneys and ADR-treated mouse kidneys 1 day, 3 days, and 14 days after ADR administration were examined for the presence of p-p38 (**Ai**) and p-Smad2 (**Bi**) by Western blot analysis. Blots were stripped and probed for β-tubulin as a loading control. Graphs (**Aii** and **Bii**) show densitometry analysis (mean ± SD) of the ratio of p-p38 and p-Smad2 to β-tubulin compared with normal saline-treated animals (assigned a normal saline treated group p-p38 or p-Smad2 to β-tubulin ration of 1). Data are means ± SD. In **Aii** and **Bii**, a: versus NS, $P < 0.05$; b: versus ADR 1 day, $P > 0.05$; c: versus ADR 1 day, $P < 0.05$; d: versus ADR 3 days, $P < 0.05$.

respectively, compared with the NS group (Figure 2B, i and ii). At days 1 and 3, the elevation of p-p38 and p-Smad2 was evident as a 1.5- and 2-fold and 0.9- and 1.1-fold increase, respectively, compared with the NS group. These results indicate that the activation of p38 MAPK occurs more rapidly than that of p-Smad2.

Effect of SB203580 and ALK5I on the Activity of p38 and p-Smad2 in ADR-Induced Nephrosis

To investigate the functional contribution of the Smad and p38 MAPK signaling pathways leading to kidney fibrosis, SB203580 (1 μg/g/24 hours) and/or ALK5I (1 μg/g/24 hours) were administered to mice with ADR-induced nephropathy. Compared with the treatment with vehicle, SB203580 alone or ALK5I alone in ADR-injected mice, combination treatment with SB203580 and ALK5I significantly reduced the activity of p38 MAPK. This was demonstrated by immunohistochemistry showing the percentage of p-ATF2-positive cells in glomeruli (Figure 3, A–E and K) and in the cortical tubulointerstitium (Figure 3, A–E and L). Immunohistochemistry was used to analyze the percentage of p-Smad2-positive cells in the glomeruli and cortical tubulointerstitium (Figure 3, F–J). Compared with the treatment of ADR-injected mice with vehicle, SB203580 alone or ALK5I alone, co-administration of both SB203580 and ALK5I also significantly reduced the activity of p-Smad2 (Figure 3, M and N).

The Effects of SB203580 and/or ALK5I Treatment on Renal Function

Mice with ADR-induced nephrosis developed significant focal and segmental glomerulosclerosis and interstitial fibrosis by 4 weeks after ADR administration, as demonstrated by PAS staining, compared with NS mice (Figure 4A). Treatment of ADR-injected mice with SB203580 or ALK5I ameliorated ADR-induced glomerulosclerosis and interstitial fibrosis [Figure 4, A (i–v), B, and C] and was associated with significantly reduced serum creatinine levels (Figure 4D) and proteinuria (Figure 4E). Furthermore, co-administration of SB203580 and ALK5I to ADR-injected mice ameliorated the progression of renal fibrosis and further reduced serum creatinine and proteinuria compared with mice administered SB203580 or ALK5I alone (Figure 4, A and E).

Effects of SB203580 and/or ALK5I on the Production of TGF-β1

Immunohistochemistry demonstrated that TGF-β1 was progressively increased with the development of ADR-induced nephropathy and was localized to renal tubular epithelial cells and interstitial cells (Figure 5A). Treatment of ADR-injected mice with SB203580 and/or ALK5I reduced the level of TGF-β1 (Figure 5A). Using enzyme-linked immunosorbent assay there was a significant up-

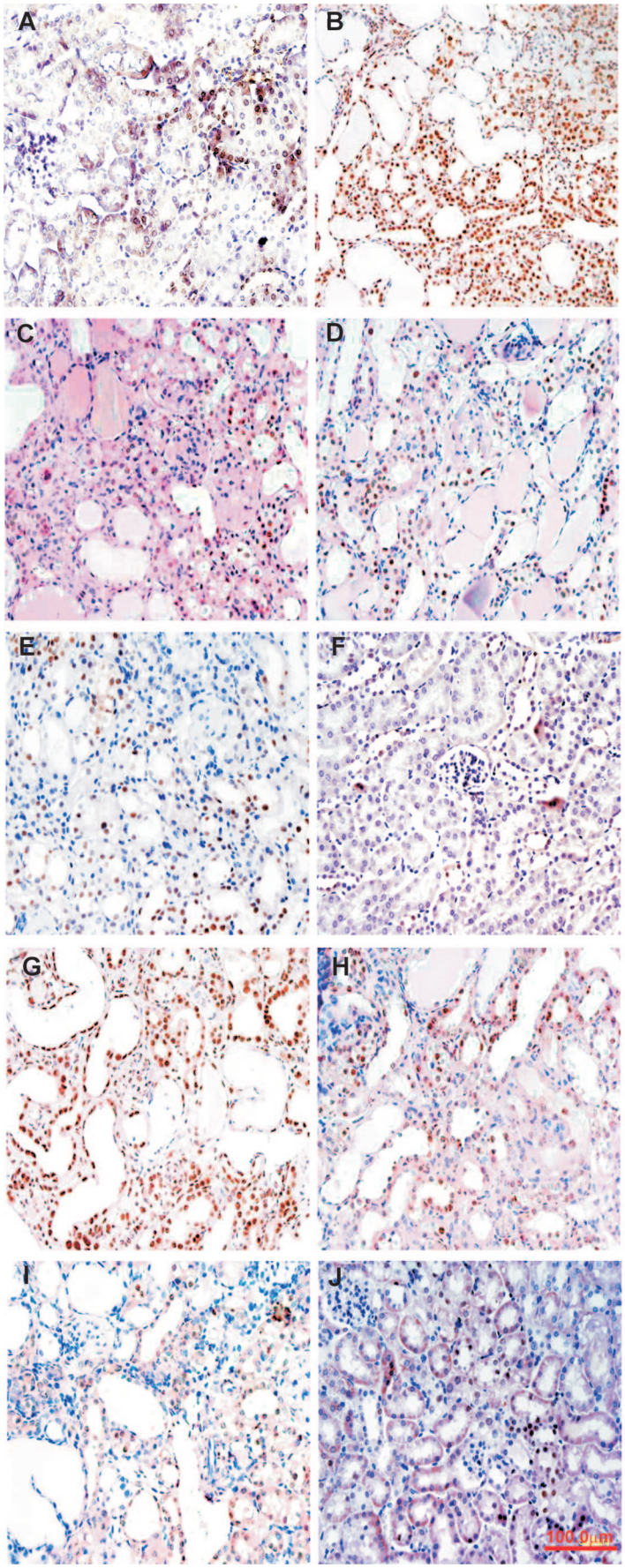

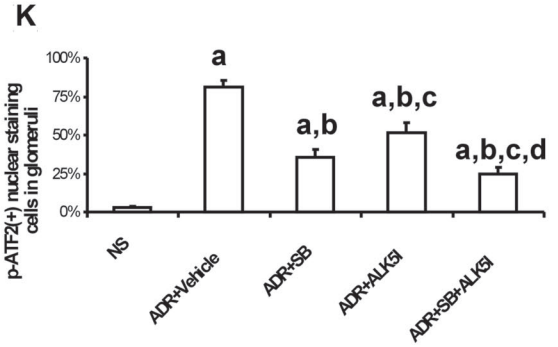

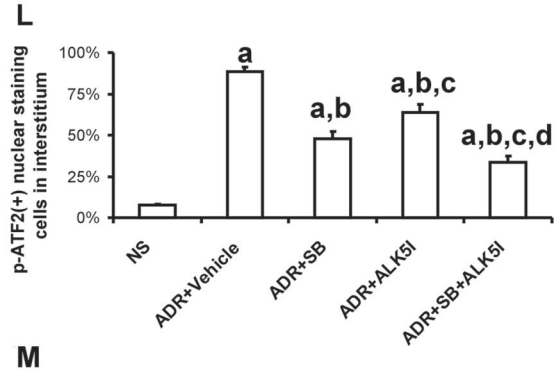

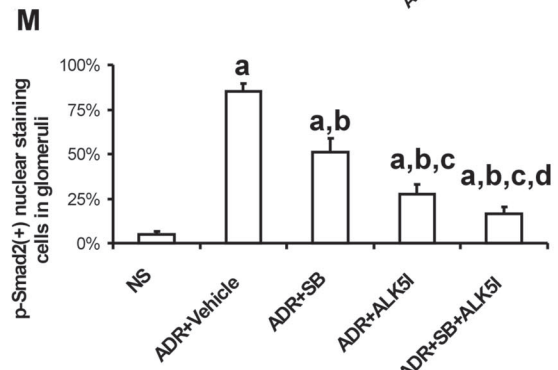

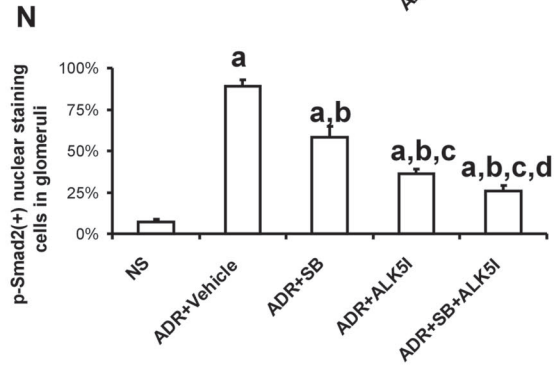

Figure 3. p-p38 MAPK and p-Smad2 blockade by SB203580 and ALK5I in ADR nephropathy. Immunohistochemical nuclear staining of p-ATF2 (brown, **A–E**) and p-Smad2 (brown, **F–J**) in glomeruli and the tubulointerstitium of NS (**A**, **F**), vehicle-treated (**B**, **G**), SB203580-treated (**C**, **H**), ALK5I-treated (**D**, **I**), and after the co-administration of SB203580 and ALK5I (**E**, **J**). **A** and **B:** In vehicle-treated animals, intrinsic renal and almost all infiltrating inflammatory cells had nuclear staining for p-ATF2 (**B**) and p-Smad2 (**G**). Reduced numbers of cells with positive nuclear staining for p-ATF2 and p-Smad2 were observed after treatment with SB203580 (**C**, **H**), ALK5I (**D**, **I**), and co-administration of SB203580 and ALK5I treatment (**E**, **J**). Graphs show the percentage of the numbers of cells with positive nuclear staining for p-ATF2 (**K**, **L**) and p-Smad2 (**M**, **N**)/total cells. Data are means ± SD. In **K–N**, a: versus NS, $P < 0.05$; b: versus ADR + vehicle, $P < 0.05$; c: versus ADR + SB, $P < 0.05$; d: versus ADR + ALK5I, $P < 0.05$. Original magnifications, ×400.

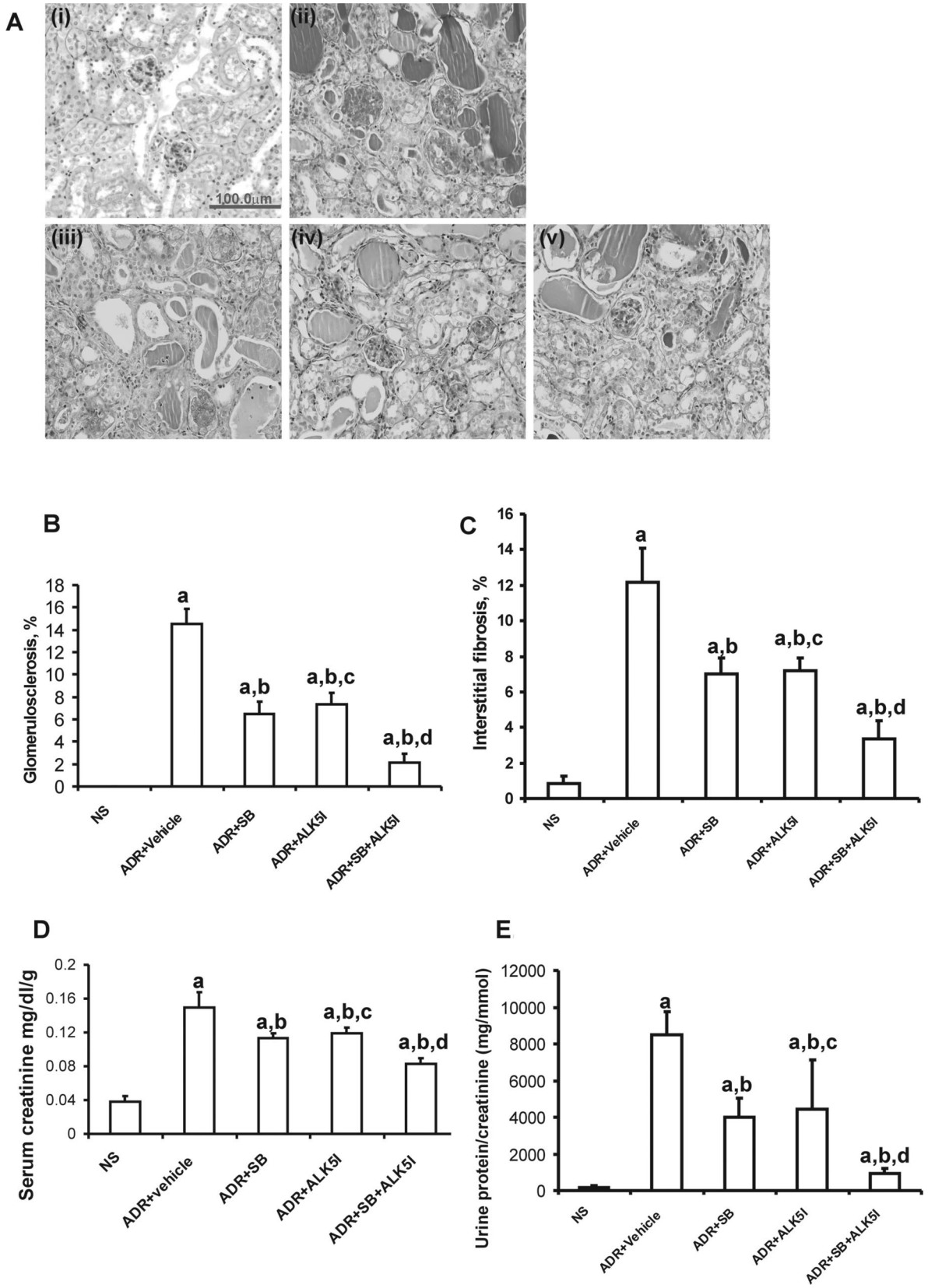

Figure 4. Effects of SB203580 and ALK5I on ADR-induced nephrosis. **A:** PAS staining on sections from mice: **i**, NS; **ii**, ADR + vehicle; **iii**, ADR + SB203580; **iv**, ADR + ALK5I; **v**, ADR + SB203580 + ALK5I. The co-administration of SB203580 and ALK5I to ADR-injected mice ameliorated the progression of renal fibrosis (**B**, **C**) and significantly reduced serum creatinine (**D**) and proteinuria (**E**), compared with mice administered SB203580 or ALK5I alone (**A**, **D**, **E**). Data are means ± SD. In **B–E**, a: versus NS, $P < 0.05$; b: versus ADR + vehicle, $P < 0.05$; c: versus ADR + SB, $P > 0.05$; d: versus ADR + SB or ADR + ALK5I, respectively, $P < 0.05$. Original magnifications, ×400.

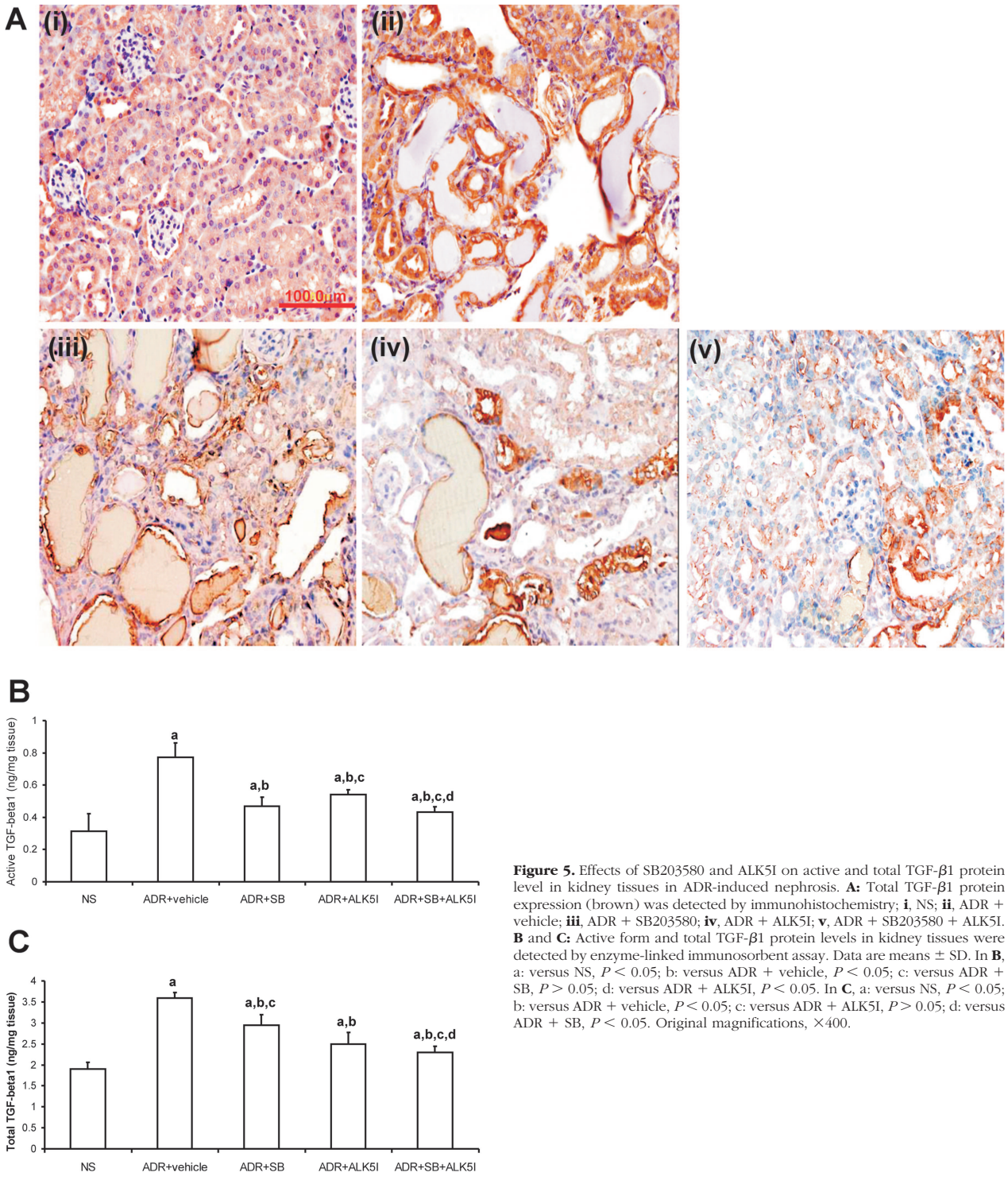

Figure 5. Effects of SB203580 and ALK5I on active and total TGF-β1 protein level in kidney tissues in ADR-induced nephrosis. **A:** Total TGF-β1 protein expression (brown) was detected by immunohistochemistry; **i**, NS; **ii**, ADR + vehicle; **iii**, ADR + SB203580; **iv**, ADR + ALK5I; **v**, ADR + SB203580 + ALK5I. **B** and **C:** Active form and total TGF-β1 protein levels in kidney tissues were detected by enzyme-linked immunosorbent assay. Data are means ± SD. In **B**, a: versus NS, $P < 0.05$; b: versus ADR + vehicle, $P < 0.05$; c: versus ADR + SB, $P > 0.05$; d: versus ADR + ALK5I, $P < 0.05$. In **C**, a: versus NS, $P < 0.05$; b: versus ADR + vehicle, $P < 0.05$; c: versus ADR + ALK5I, $P > 0.05$; d: versus ADR + SB, $P < 0.05$. Original magnifications, ×400.

regulation of active and total TGF-β1 production in ADR-injected mice compared with NS mice (Figure 5, B and C). ADR-injected mice administered SB203580, ALK5I, or SB203580 + ALK5I, respectively, had significantly reduced active and total TGF-β1 production compared with ADR-injected mice treated with vehicle (Figure 5, B and C). Furthermore, when active TGF-β1 production was measured, there was a significant difference between treatments with SB203580 alone or co-administration of SB203580 + ALK5I and ALK5I alone. However, in total TGF-β1 production, there was a significant difference between treatments with ALK5I alone or co-administration of SB203580 + ALK5I and SB203580 alone. Only co-administration of SB203580 + ALK5I reduced both active TGF-β1 and total TGF-β1 production when compared with vehicle, SB203580 alone, or ALK5I alone in ADR-injected mice (Figure 5, B and C).

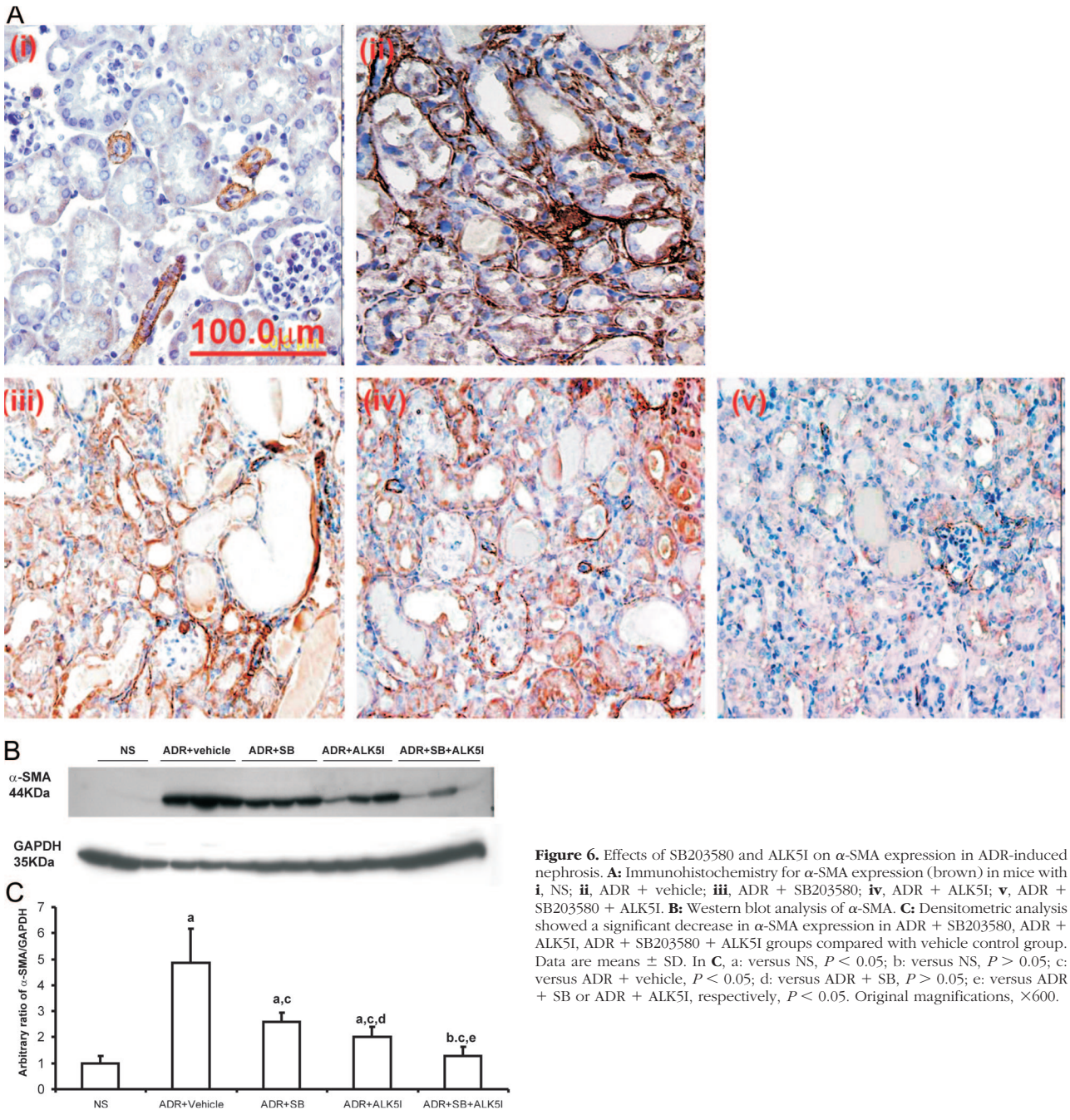

Figure 6. Effects of SB203580 and ALK5I on α-SMA expression in ADR-induced nephrosis. **A:** Immunohistochemistry for α-SMA expression (brown) in mice with **i**, NS; **ii**, ADR + vehicle; **iii**, ADR + SB203580; **iv**, ADR + ALK5I; **v**, ADR + SB203580 + ALK5I. **B:** Western blot analysis of α-SMA. **C:** Densitometric analysis showed a significant decrease in α-SMA expression in ADR + SB203580, ADR + ALK5I, ADR + SB203580 + ALK5I groups compared with vehicle control group. Data are means ± SD. In **C**, a: versus NS, $P < 0.05$; b: versus NS, $P > 0.05$; c: versus ADR + vehicle, $P < 0.05$; d: versus ADR + SB, $P > 0.05$; e: versus ADR + SB or ADR + ALK5I, respectively, $P < 0.05$. Original magnifications, ×600.

Treatment with SB203580 and/or ALK5I on the Accumulation of Myofibroblasts

Immunohistochemistry demonstrated the level of α-smooth muscle actin (α-SMA) expression at 4 weeks in ADR-injected mice treated with SB203580 or ALK5I was less than in ADR-injected mice treated with vehicle. Co-administration of SB203580 and ALK5I to ADR-injected mice further decreased α-SMA immunostaining (Figure 6A) This was confirmed by Western blot analysis in which a 59% (SB203580) and 74% (ALK5I) decrease in α-SMA expression was observed, compared with treatment with vehicle in ADR-injected mice (Figure 6, B and C). The co-administration of SB203580 and ALK5I to ADR-injected mice had an additive effect on the down-regulation of α-SMA expression (93%) compared with treatment with vehicle in ADR-injected mice (Figure 6, B and C).

p38 MAPK and TGF/Smad Signaling Pathways Coordinate ECM Synthesis

Western blot analysis showed that the separate administration of SB203580 or ALK5I to ADR-injected mice dramatically inhibited collagen type IV expression by 59%

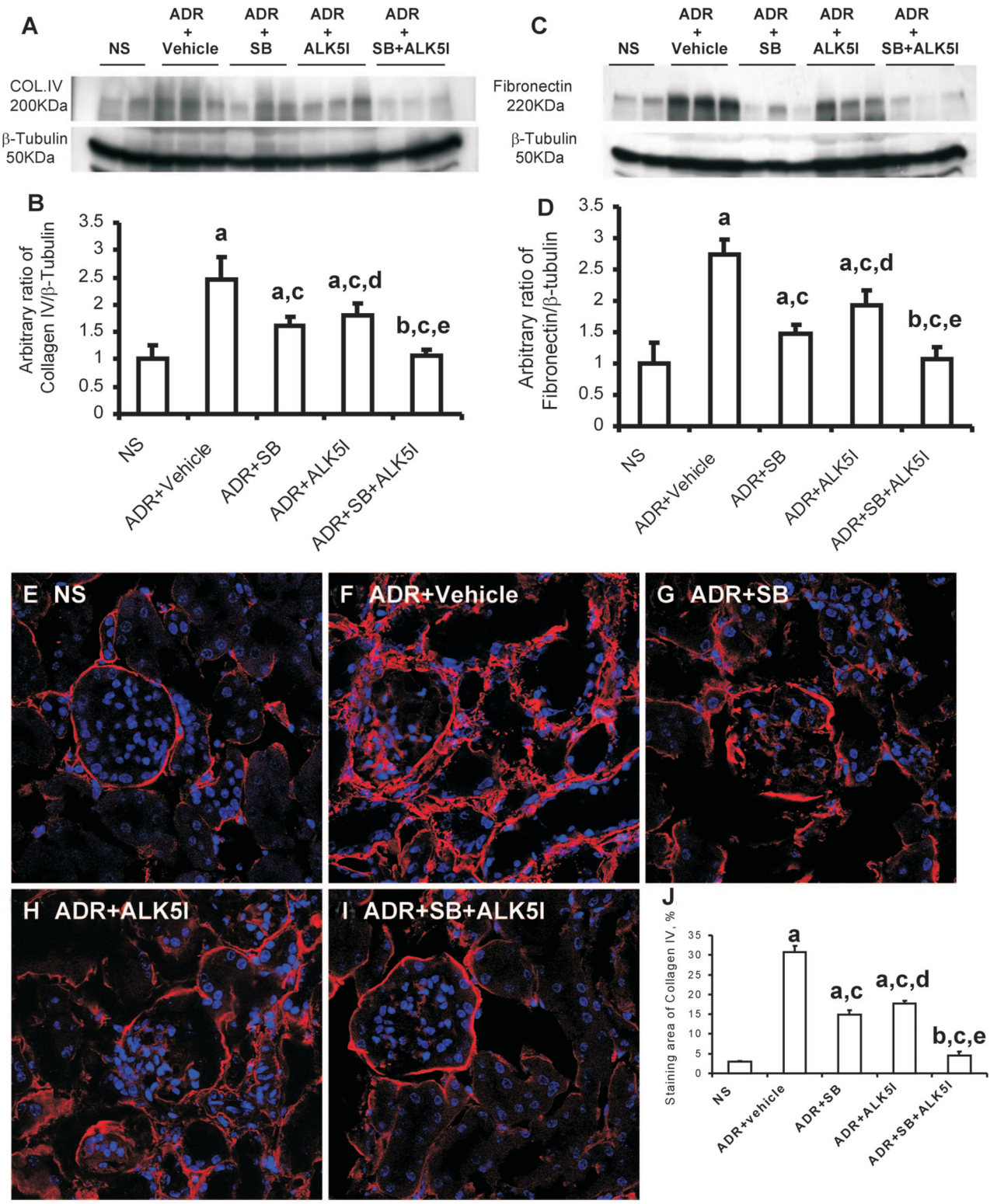

Figure 7. Western blot analysis of the effects of SB203580 and/or ALK5I on collagen IV (**A**) and fibronectin (**B**) deposition in ADR-induced nephrosis. Densitometric analysis of the ratios of collagen type IV/β-tubulin (**B**) and fibronectin/β-tubulin (**D**) (assigned a normal saline-treated group collagen IV or fibronectin to β-tubulin ration of 1). Confocal microscopic analysis of the effects of SB203580 and ALK5I on collagen IV deposition in ADR-induced nephrosis: **E:** NS; **F:** ADR + vehicle; **G:** ADR + SB; **H:** ADR + ALK5I; and **I:** ADR + SB + ALK5I groups. **J:** Quantification of the production of collagen IV. Data are means ± SD. In **B**, **D**, and **J**, a: versus NS, $P < 0.05$; b: versus NS, $P > 0.05$; c: versus ADR + vehicle, $P < 0.05$; d: versus ADR + SB, $P > 0.05$; e: versus ADR + SB or ADR + ALK5I, respectively, $P < 0.05$.

and 46%, respectively, and fibronectin expression by 67% and 45%, respectively, compared with treatment with vehicle (Figure 7, A–D). Co-administration of SB203580 and ALK5I further decreased both the expression of collagen type IV (93%) and fibronectin (95%) in mice with ADR-induced nephropathy compared with ve-

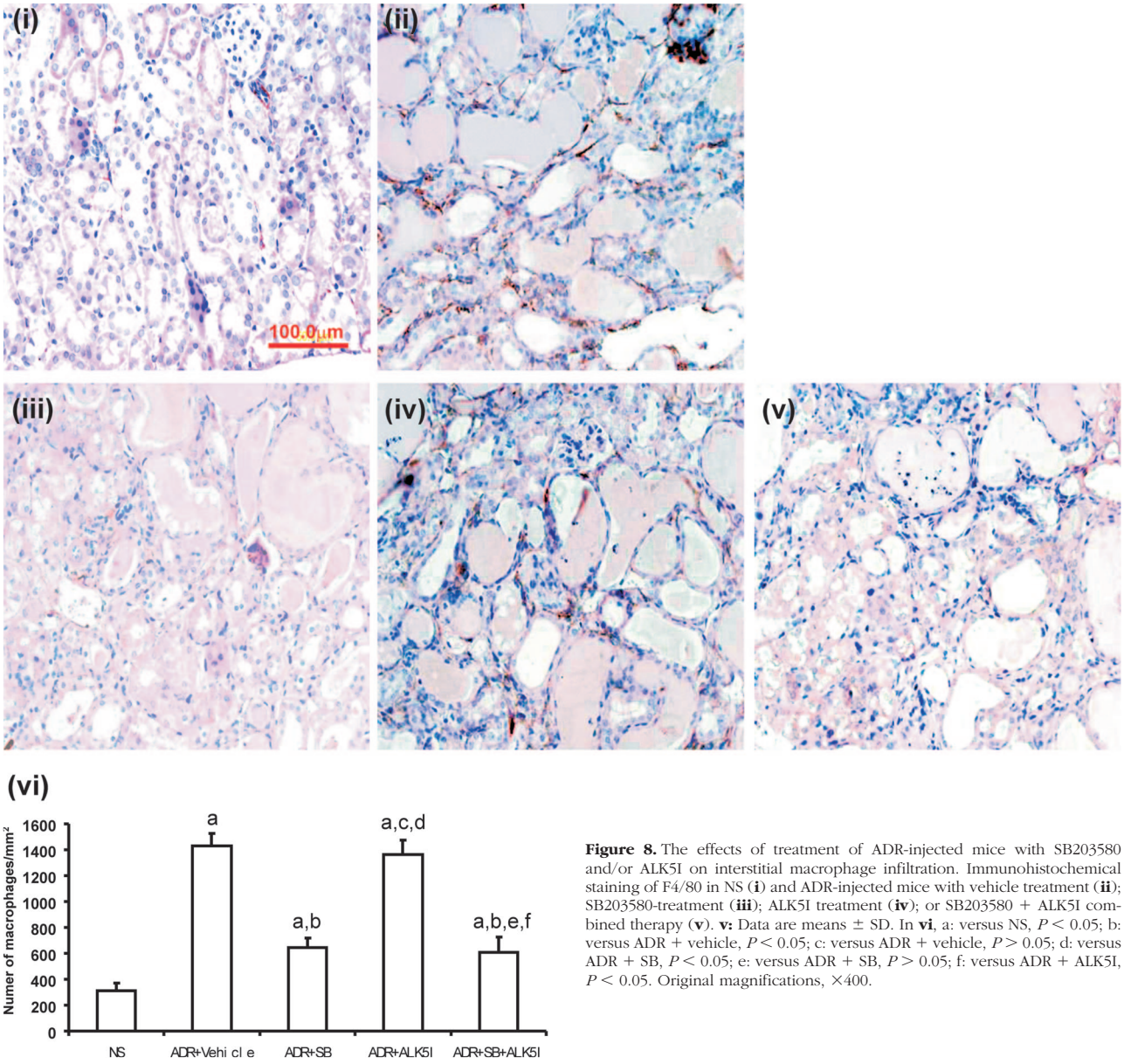

Figure 8. The effects of treatment of ADR-injected mice with SB203580 and/or ALK5I on interstitial macrophage infiltration. Immunohistochemical staining of F4/80 in NS (**i**) and ADR-injected mice with vehicle treatment (**ii**); SB203580-treatment (**iii**); ALK5I treatment (**iv**); or SB203580 + ALK5I combined therapy (**v**). **v:** Data are means ± SD. In **vi**, a: versus NS, $P < 0.05$; b: versus ADR + vehicle, $P < 0.05$; c: versus ADR + vehicle, $P > 0.05$; d: versus ADR + SB, $P < 0.05$; e: versus ADR + SB, $P > 0.05$; f: versus ADR + ALK5I, $P < 0.05$. Original magnifications, ×400.

hicle treatment (Figure 7, B and D). The confocal microscopy analysis for the deposition of collagen IV (Figure 7, E–J) also confirmed the results demonstrated by Western blotting.

SB203580, but Not ALK5I, Can Inhibit Macrophage Infiltration in ADR-Induced Nephropathy

The administration of ALK5I to ADR-injected mice did not lead to an alteration in the number of infiltrating interstitial macrophages compared with ADR-injected mice with vehicle treatment (Figure 8). However, there was a 70 and 74% decrease in the number of infiltrating interstitial macrophages when ADR-injected mice were treated with SB203580 or the combined therapy of SB203580 and ALK5I, respectively (Figure 8, i–vi). The number of interstitial CD4 and CD8 T lymphocytes was not found to be altered in ADR-injected mice treated with SB203580, ALK5I, or SB203580 + ALK5I (data not shown).

Discussion

The present study demonstrates that a combined therapy using SB203580 and ALK5I can attenuate renal injury and reduce the progression of ADR-induced nephropathy, compared with the separate administration of these factors. The co-administration of SB203580 and ALK5I afforded marked renoprotection as evidenced by the reduced development of glomerulosclerosis and reduced interstitial matrix expansion, decreased urine protein and serum creatine levels, decreased active and total TGF-β1 production, and reduced myofibroblast accumulation leading to down-regu-

lated expression of collagen type IV and fibronectin. In addition, decreased activities of p38 and Smad2 were observed in the kidneys from ADR-injected mice when co-administered SB203580 and ALK5I. Interestingly, the separate administration of SB203580 or combined administration of SB203580 and ALK5I to ADR mice resulted in a decrease in the number of infiltrating macrophages in the cortical interstitium compared with vehicle or ALK5I administration alone. These results demonstrate that p38 MAPK and TGF-β/Smad2 signaling pathways, although distinct, play a coordinated role in the progression of renal fibrosis and the co-administration may provide a new therapeutic strategy for patients with chronic progressive renal diseases.

There is growing evidence that inflammation and fibrosis play critical roles in the progression of renal disease.[24] The role of the p38 MAPK signaling has been extensively studied because mammalian p38 MAPK was identified and implicated in inflammation.[25,26] p38 MAPK activation has been demonstrated in human and experimental diabetic nephropathy.[9] The activation of p38 MAPK in intrinsic renal cells and infiltrating leukocytes has been found to correlate with renal dysfunction and histopathology in human glomerulonephritis.[10] The interference of this pathway can ameliorate renal fibrosis in a rat model of unilateral ureteral obstruction and anti-glomerular basement membrane disease.[12,13] Koshikawa and colleagues[27] demonstrated that pretreatment with p38 MAPK inhibitor can reduce podocyte injury and proteinuria in ADR or puromycin-induced experimental nephrotic syndrome.

p38 MAPK activation is a key modulator in the progression of renal disease. However, complete inhibition of the p38 MAPK pathway can result in the activation of other signaling pathways. For example, the total ablation of p38 MAPK has been shown to worsen kidney function in a rat remnant kidney model.[28] In our study, the production of p-ATF, an intermediate in the p38 MAPK pathway, is diminished by 50% when administered at a dose of 1 μg/g/day SB203580. In contrast p-ATF production is further reduced to ~80% when SB203580 is administered in combination with 1.0 μg/g/day ALK5I.

The level of TGF-β1 expression is a critical determinant of the severity of renal fibrosis.[29] Isaka and colleagues[30] demonstrated that the overexpression of TGF-β1, by the introduction of exogenous TGF-β1 cDNA to the kidney, leads to the development of glomerulosclerosis. Furthermore, the obstruction of TGF-β1 by adenovirus-mediated TGF-β type II receptor gene transfer in the early stage of anti-GBM nephritis ameliorates the clinical and histological progression of disease.[19] One of the most important profibrotic effects of TGF-β1 is autoinduction in a variety of mesenchymal cell types, which may be responsible for sustaining or amplifying TGF-β1 response in an autocrine or paracrine manner.[31] Our study demonstrated that ALK5I significantly inhibited TGF-β1 production in ADR-induced nephropathy, giving further weight to the hypothesis that interference of TGF-β1/Smad signaling pathway can reduce renal fibrosis. The possible pathways mediating renal TGF-β1 activation include protease, thrombospondin-1, reactive oxygen species, and low pH.[32] In our study, SB203580 administration significantly inhibited the production of the active form of TGF-β1, suggesting that inflammation can mediate renal TGF-β1 activation. We demonstrated that the co-administration of SB203580 and ALK5I not only inhibits TGF-β1 autoinduction but also the conversion of TGF-β1 from the latent to active form. Our data imply that both the p38 MAPK and TGF-β1/Smad signaling pathways contribute fundamentally in an additive manner to both the active and total TGF-β1 production in ADR-induced nephropathy. This is a central mechanism in our study demonstrating that blockade of p38 MAPK and TGF-β1/Smad signaling pathways can orchestrate the retardation of renal fibrosis.

Recent *in vitro* studies have shown that advanced glycation end products can activate the Smad signaling pathway independent of TGF-β1 through a MAPK-Smad cross-talk signaling pathway mechanism in mesangial cells, tubular epithelial cells, and vascular smooth muscle cells.[23] Angiotensin (ATII) can also activate the Smad2 signaling pathway through a p38 MAPK-Smad2 cross-talk mechanism *in vitro* and *in vivo*.[33] The intracellular kinase mitogen-activated protein kinase kinase kinase-1 (MEKK-1), an upstream activator of the stress-activated protein kinase/c-Jun N-terminal kinase pathway, can participate in Smad2-dependent transcriptional events in endothelial cells.[34,35] However, Smad2 and Smad3 are distinct proteins whereby only Smad3 can directly bind to DNA to regulate gene transcription.[36]

The accumulation of myofibroblasts is consistent with the severity of the renal fibrosis and serves as a predictor of the outcome of renal progressive fibrosis in human IgA nephropathy and glomerulonephritis.[37,38] The co-administration of SB203580 and ALK5I significantly reduced α-SMA-positive myofibroblast accumulation and also significantly decreased total and active TGF-β1 production. TGF-β1 is a strong inducer of epithelial-myofibroblast and fibroblast-myofibroblast transition.[38,39] The blockade of p38 MAPK and TGF-β/Smad signaling results in down-regulation of TGF-β1 synthesis and reduced active form of TGF-β1 formation, which may lead to an inhibition of myofibroblast transition and accumulation resulting in an amelioration of renal fibrosis.

TGF-β1 can activate the canonical Smad-mediated signaling pathway and non-Smad signaling pathway, such as TGF-β1-activated kinase-1 (TAK1) and p38 MAPK. Studies show that TGF-β1 can activate p38 MAPK via TAK1 and lead to phosphorylation of activating transcription factor-2 (p-ATF-2), which then directly binds to Smad3/4 hetero-oligomers to regulate transcription of targeted genes.[40] It suggests p38 MAPK and Smads transduce distinct, parallel signals to the nucleus, where they synergistically converge and enhance their regulating cellular activities.[41] In our study, co-administration of SB203580 and ALK5I further decreased synthesis of ECM components, including α-SMA, collagen IV, and fibronectin, in ADR-injected mice compared with SB203580 alone or ALK5I alone. This suggests that both p38 MAPK and TGF-β/Smad signaling pathways control the synthesis of different components of ECM in an additive manner.

The development of renal fibrosis is a complicated process with a variety of cellular and molecular mediators

interacting in concert. Cytokines, growth factors, signaling pathways, and the renin-angiotensin system have been reported to play important roles in the progression of tubulointerstitial fibrosis leading to a decline in renal function. In the present study, treatment with the p38 MAPK inhibitor SB203580 and the TGF-β1/Smad inhibitor ALK5I was found to significantly retard the progression of renal fibrosis, compared with vehicle-injected mice with/without SB203580 and ALK5I alone. Despite a marked improvement in renal structure and functional recovery, administration of SB203580 and ALK5I to ADR-injected mice did not completely halt the progression of renal fibrosis. This suggests that other signaling pathways and downstream mediators are involved in renal inflammation and the pathogenesis of fibrotic damage. Further studies are required to elucidate the exact roles of other signaling pathways, cytokines, and the renin-angiotensin system to develop combination therapies to further attenuate renal fibrosis and inflammation.

The present study demonstrates for the first time that p38 MAPK and TGF-β/Smad signaling pathways are activated and can contribute to renal fibrosis independently and in an additive manner. The administration of both SB203580 and ALK5I to mice with ADR nephropathy was found to inhibit the active and total form of TGF-β1, reduce ECM synthesis and myofibroblast accumulation, reduce urine protein and serum creatinine levels, and inhibit macrophage infiltration without obvious side effects. The coordinated interplay of the p38 MAPK and TGF-β/Smad signaling pathways may have potential clinical applications for the treatment of renal fibrosis.

Acknowledgments

We thank the members of the Renal Regeneration Consortium for their support.

References

1. Ono K, Han J: The p38 signal transduction pathway activation and function. Cell Signal 2000, 12:1–13
2. New L, Han J: The p38 MAP kinase pathway and its biological function. Trends Cardiovasc Med 1998, 8:220–228
3. Ichijo H, Nishida E, Irie K, ten Dijke P, Saitoh M, Moriguchi T, Takagi M, Matsumoto K, Miyazono K, Gotoh Y: Induction of apoptosis by ASK1, a mammalian MAPKKK that activates SAPK/JNK and p38 signaling pathways. Science 1997, 275:90–94
4. Raingeaud J, Gupta S, Rogers JS, Dickens M, Han J, Ulevitch RJ, Davis RJ: Pro-inflammatory cytokines and environmental stress cause p38 mitogen-activated protein kinase activation by dual phosphorylation on tyrosine and threonine. J Biol Chem 1995, 270:7420–7426
5. Yoshinari D, Takeyoshi I, Koibuchi Y, Matsumoto K, Kawashima Y, Koyama T, Ohwada S, Morishita Y: Related articles, effects of a dual inhibitor of tumor necrosis factor-alpha and interleukin-1 on lipopolysaccharide-induced lung injury in rats: involvement of the p38 mitogen-activated protein kinase pathway. Crit Care Med 2001, 29:628–634
6. Geng Y, Valbracht J, Lotz M: Selective activation of the mitogen-activated protein kinase subgroups c-Jun NH2 terminal kinase and p38 by IL-1 and TNF in human articular chondrocytes. J Clin Invest 1996, 98:2425–2430
7. Furuichi K, Wada T, Iwata Y, Sakai N, Yoshimoto K, Kobayashi K, Mukaida N, Matsushima K, Yokoyama H: Administration of FR167653, a new anti-inflammatory compound, prevents renal ischaemia/reperfusion injury in mice. Nephrol Dial Transplant 2002, 17:399–407
8. Hommes D, van den Blink B, Plasse T, Bartelsman J, Xu C, Macpherson B, Tytgat G, Peppelenbosch M, Van Deventer S: Inhibition of stress-activated MAP kinases induces clinical improvement in moderate to severe Crohn's disease. Gastroenterology 2002, 122:7–14
9. Adhikary L, Chow F, Nikolic-Paterson DJ, Stambe C, Dowling J, Atkins RC, Tesch GH: Abnormal p38 mitogen-activated protein kinase signalling in human and experimental diabetic nephropathy. Diabetologia 2004, 47:1210–1222
10. Stambe C, Nikolic-Paterson DJ, Hill PA, Dowling J, Atkins RC: p38 mitogen-activated protein kinase activation and cell localization in human glomerulonephritis: correlation with renal injury. J Am Soc Nephrol 2004, 15:326–336
11. Lee JC, Kassis S, Kumar S, Badger A, Adams JL: p38 mitogen-activated protein kinase inhibitors—mechanisms and therapeutic potentials. Pharmacol Ther 2003, 82:389–397
12. Stambe C, Atkins RC, Tesch GH, Kapoun AM, Hill PA, Schreiner GF, Nikolic-Paterson DJ: Blockade of p38alpha MAPK ameliorates acute inflammatory renal injury in rat anti-GBM glomerulonephritis. J Am Soc Nephrol 2003, 14:338–351
13. Stambe C, Atkins RC, Tesch GH, Masaki T, Schreiner GF, Nikolic-Paterson DJ: The role of p38alpha mitogen-activated protein kinase activation in renal fibrosis. J Am Soc Nephrol 2004, 15:370–379
14. Border WA, Okuda S, Languino LR, Sporn MB, Ruoslahti E: Suppression of experimental glomerulonephritis by antiserum against transforming growth factor beta 1. Nature 1990, 346:371–374
15. Peters H, Noble NA, Border WA: Transforming growth factor-beta in human glomerular injury. Curr Opin Nephrol Hypertens 1997, 6:389–393
16. Wang W, Koka V, Lan HY: Transforming growth factor-beta and Smad signalling in kidney diseases. Nephrology (Carlton) 2005, 10:48–56
17. Fukasawa H, Yamamoto T, Suzuki H, Togawa A, Ohashi N, Fujigaki Y, Uchida C, Aoki M, Hosono M, Kitagawa M, Hishida A: Treatment with anti-TGF-beta antibody ameliorates chronic progressive nephritis by inhibiting Smad/TGF-beta signaling. Kidney Int 2004, 65:63–74
18. Lan HY, Mu W, Tomita N, Huang XR, Li JH, Zhu HJ, Morishita R, Johnson RJ: Inhibition of renal fibrosis by gene transfer of inducible Smad7 using ultrasound-microbubble system in rat UUO model. J Am Soc Nephrol 2003, 14:1535–1548
19. Zhou A, Ueno H, Shimomura M, Tanaka R, Shirakawa T, Nakamura H, Matsuo M, Iijima K: Blockade of TGF-beta action ameliorates renal dysfunction and histologic progression in anti-GBM nephritis. Kidney Int 2003, 64:92–101
20. Grygielko ET, Martin WM, Tweed C, Thornton P, Harling J, Brooks DP, Laping NJ: Inhibition of gene markers of fibrosis with a novel inhibitor of transforming growth factor-beta type I receptor kinase in puromycin-induced nephritis. J Pharmacol Exp Ther 2005, 313:943–951
21. Wang Y, Wang YP, Tay YC, Harris DC: Progressive adriamycin nephropathy in mice: sequence of histologic and immunohistochemical events. Kidney Int 2000, 58:1797–1804
22. Vleming LJ, Baelde JJ, Westendorp RG, Daha MR, van Es LA, Bruijn JA: The glomerular deposition of PAS positive material correlates with renal function in human kidney diseases. Clin Nephrol 1997, 47:158–167
23. Li JH, Huang XR, Zhu HJ, Oldfield M, Cooper M, Truong LD, Johnson RJ, Lan: HY Advanced glycation end products activate Smad signaling via TGF-beta-dependent and independent mechanisms: implications for diabetic renal and vascular disease. FASEB J 2004, 18:176–178
24. Noronha IL, Fujihara CK, Zatz R: The inflammatory component in progressive renal disease—are interventions possible? Nephrol Dial Transplant 2002, 17:363–368
25. Han J, Lee JD, Bibbs L, Ulevitch RJ: A MAP kinase targeted by endotoxin and hyperosmolarity in mammalian cells. Science 1994, 265:808–811
26. Badger AM, Bradbeer JN, Votta B, Lee JC, Adams JL, Griswold DE: Pharmacological profile of SB 203580, a selective inhibitor of cytokine suppressive binding protein/p38 kinase, in animal models of arthritis, bone resorption, endotoxin shock and immune function. J Pharmacol Exp Ther 1996, 279:1453–1461
27. Koshikawa M, Mukoyama M, Mori K, Suganami T, Sawai K, Yoshioka T, Nagae T, Yokoi H, Kawachi H, Shimizu F, Sugawara A, Nakao K: Role of p38 mitogen-activated protein kinase activation in podocyte injury and proteinuria in experimental nephrotic syndrome. J Am Soc Nephrol 2005, 16:2690–2701

28. Ohashi R, Nakagawa T, Watanabe S, Kanellis J, Almirez RG, Schreiner GF, Johnson RJ: Inhibition of p38 mitogen-activated protein kinase augments progression of remnant kidney model by activating the ERK pathway. Am J Pathol 2004, 64:477–485
29. Border WA, Noble NA: TGF-beta in kidney fibrosis: a target for gene therapy. Kidney Int 1997, 51:1388–1396
30. Isaka Y, Fujiwara Y, Ueda N, Kaneda Y, Kamada T, Imai E: Glomerulosclerosis induced by in vivo transfection of transforming growth factor-beta or platelet-derived growth factor gene into the rat kidney. J Clin Invest 1993, 92:2597–2601
31. Mori Y, Ishida W, Bhattacharyya S, Li Y, Platanias LC, Varga J: Selective inhibition of activin receptor-like kinase 5 signaling blocks profibrotic transforming growth factor beta responses in skin fibroblasts. Arthritis Rheum 2002, 50:4008–4012
32. Koli K, Saharinen J, Hyytiainen M, Penttinen C, Keski-Oja J: Latency, activation, and binding proteins of TGF-beta. Microsc Res Tech 2001, 52:354–362
33. Rodriguez-Vita J, Sanchez-Lopez E, Esteban V, Ruperez M, Egido J, Ruiz-Ortega M: Angiotensin II activates the Smad pathway in vascular smooth muscle cells by a transforming growth factor-beta-independent mechanism. Circulation 2005, 111:2509–2517
34. Brown JD, DiChiara MR, Anderson KR, Gimbrone Jr MA, Topper JN: MEKK-1, a component of the stress (stress-activated protein kinase/c-Jun N-terminal kinase) pathway, can selectively activate Smad2-mediated transcriptional activation in endothelial cells. J Biol Chem 1999, 274:8797–8805
35. Datto MB, Frederick JP, Pan L, Borton AJ, Zhuang Y, Wang XF: Targeted disruption of Smad3 reveals an essential role in transforming growth factor-mediated signal transduction. Mol Cell Biol 1999, 19:2495–2504
36. Zhang G, Moorhead P, El Nahas AM: Myofibroblasts and the progression of experimental glomerulonephritis. Exp Nephrol 1995, 3:308–318
37. Goumenos DS, Brown CB, Shortland J, el Nahas AM: Myofibroblasts, predictors of progression of mesangial IgA nephropathy? Nephrol Dial Transplant 1994, 9:1418–1425
38. Fan JM, Ng YY, Hill PA, Nikolic-Paterson DJ, Mu W, Atkins RC, Lan HY: Transforming growth factor-beta regulates tubular epithelial-myofibroblast transdifferentiation in vitro. Kidney Int 1999, 56:1455–1467
39. Hu B, Wu Z, Phan SH: Smad3 mediates transforming growth factor-β-induced α-smooth muscle actin expression. Am J Respir Cell Mol Biol 2003, 29:397–404
40. Tsukada S, Westwick JK, Ikejima K, Sato N, Rippe RA: SMAD and p38 MAPK signaling pathways independently regulate alpha1(I) collagen gene expression in unstimulated and transforming growth factor-beta-stimulated hepatic stellate cells. J Biol Chem 2005, 280:10055–10064
41. Hayes SA, Huang X, Kambhampati S, Platanias LC, Bergan RC: p38 MAP kinase modulates Smad-dependent changes in human prostate cell adhesion. Oncogene 2003, 22:4841–4850